




The COVID-19 Pandemic Sparked Off a Large-Scale Outbreak of Carbapenem-Resistant *Acinetobacter baumannii* from the Endemic Strains at an Italian Hospital

Greta Petazzoni,^a Greta Bellinzona,^b Cristina Merla,^a Marta Corbella,^a Vincenzina Monzillo,^{a,c} Ørjan Samuelsen,^{d,e} Jukka Corander,^{f,g} Davide Sasseria,^b  Stefano Gaiarsa,^a Patrizia Cambieri^a

^aMicrobiology and Virology Unit, Fondazione IRCCS Policlinico San Matteo, Pavia, Italy

^bDepartment of Biology and Biotechnology, University of Pavia, Pavia, Italy

^cDepartment of Internal Medicine and Medical Therapy, University of Pavia, Pavia, Italy

^dNorwegian National Advisory Unit on Detection of Antimicrobial Resistance, Department of Microbiology and Infection Control, University Hospital of North Norway, Tromsø, Norway

^eInstitute of Pharmacy, Faculty of Health Sciences, UiT The Arctic University of Norway, Tromsø, Norway

^fDepartment of Biostatistics, University of Oslo, Oslo, Norway

^gDepartment of Mathematics and Statistics, University of Helsinki, Helsinki, Finland

Greta Petazzoni and Greta Bellinzona contributed equally to this article. The order was determined by the corresponding author after negotiation.

ABSTRACT *Acinetobacter baumannii* is a nosocomial pathogen that poses a serious threat due to the rise of incidence of multidrug-resistant (MDR) strains. During the COVID-19 pandemic, MDR *A. baumannii* clones have caused several outbreaks worldwide. Here, we describe a detailed investigation of an MDR *A. baumannii* outbreak that occurred at Policlinico San Matteo (Pavia, Italy). A total of 96 *A. baumannii* strains, isolated between January and July 2020 from 41 inpatients (both SARS-CoV-2 positive and negative) in different wards, were characterized by phenotypic and genomic analyses combining Illumina and Nanopore sequencing. Antibiotic susceptibility testing revealed that all isolates were resistant to carbapenems, and the sequence analysis attributed this to the carbapenemase gene *bla*_{OXA-23}. Virulence factor screening unveiled that all strains carried determinants for biofilm formation, while plasmid analysis revealed the presence of two plasmids, one of which was ~100 kbp long and encoded a phage sequence. A core genome-based phylogeny was inferred to integrate outbreak strain genomes with background genomes from public databases and the local surveillance program. All strains belonged to the globally disseminated sequence type 2 (ST2) clone and were mainly divided into two clades. Isolates from the outbreak clustered with surveillance isolates from 2019, suggesting that the outbreak was caused by two strains that were already circulating in the hospital before the start of the pandemic. The intensive spread of *A. baumannii* in the hospital was enhanced by the extreme emergency situation of the first COVID-19 pandemic wave that resulted in reduced attention to infection prevention and control practices.

IMPORTANCE The COVID-19 pandemic, especially during the first wave, posed a great challenge to the hospital management and generally promoted nosocomial pathogen dissemination. MDR *A. baumannii* can easily spread and persist for a long time on surfaces, causing outbreaks in health care settings. Infection prevention and control practices, epidemiological surveillance, and microbiological screening are fundamental in order to control such outbreaks. Here, we sequenced the genomes of 96 isolates from an outbreak of MDR *A. baumannii* strains using both short- and long-read technology in order to reconstruct the outbreak events in fine detail. The sequence data demonstrated that two endemic clones of MDR *A. baumannii* were the source of this large hospital outbreak during the first COVID-19 pandemic wave, confirming the

Editor Philip N. Rather, Emory University School of Medicine

Copyright © 2023 Petazzoni et al. This is an open-access article distributed under the terms of the [Creative Commons Attribution 4.0 International license](https://creativecommons.org/licenses/by/4.0/).

Address correspondence to Stefano Gaiarsa, s.gaiarsa@smatteo.pv.it.

The authors declare no conflict of interest.

Received 5 November 2022

Accepted 1 March 2023

Published 23 March 2023

effect of COVID-19 emergency disrupting the protection provided by the use of the standard prevention procedures.

KEYWORDS *Acinetobacter baumannii*, COVID-19, Illumina, Nanopore, outbreak, phylogeny, multidrug resistance, plasmids

A *Acinetobacter baumannii* is an opportunistic Gram-negative pathogen most frequently associated with health care-associated infections (HAIs). This pathogen is a member of the ESKAPE group, despite causing only 2% of HAIs (1), due to its virulence and the substantial prevalence of antibiotic resistance.

A. baumannii can evolve rapidly by acquiring determinants of resistance to a wide range of antibiotics (including front-line agents like carbapenems). Multidrug-resistant (MDR) strains are increasingly isolated in hospitals worldwide; this is a critical issue in southern Europe, especially in Italy, where the percentage of carbapenem-resistant *A. baumannii* (CRAB) strains during 2020 was 80.8% (2). In conjunction with antibiotic resistance, *A. baumannii* is concerning because of its exceptional capability to persist for long periods in the environment, even in the hospital setting, aided by biofilm production. This persistence on abiotic and biotic surfaces leads to chronic infections and facilitates its spread (3), especially in intensive care units (ICUs) (4). Indeed, *A. baumannii* infections are typically related to medical equipment such as catheters and ventilators (i.e., pneumonia and bloodstream infections), while urinary infections and those affecting skin, soft tissues, and surgical sites are less common (5). In light of this, the World Health Organization included MDR *A. baumannii* in the critical group, a list of bacteria that pose the greatest threat to human health and for which the development of novel antibiotics is urgently needed (6).

The COVID-19 pandemic has been posing an arduous challenge for hospitals worldwide, especially in the early period. The increasing COVID-19-related hospitalizations led to shortages in personnel, personal protective equipment, and medical equipment. These, in turn, often resulted in the impossibility of maintaining strict infection prevention and control (IPC) practices and, consequently, in an increase in bacterial and fungal infections. In fact, several *A. baumannii* outbreaks have been described during the first pandemic wave worldwide; e.g., in references 7 and 8. Fondazione IRCCS Policlinico San Matteo (Pavia, Italy) played a key role in the management of the COVID-19 pandemic in North Italy, especially during the first wave, being one of the largest hospitals (~900 beds) in the Lombardy region. An active genomic surveillance program and IPC containment strategies for ESKAPE pathogens were already in place in the hospital before COVID-19. Thanks to surveillance measures, the prevalence of *A. baumannii* in the 2018–2019 biennium was less than one isolate per 1,000 days of hospitalization. However, during the first wave of COVID-19, a large outbreak of MDR *A. baumannii* emerged (~2.8 isolates/1,000 days of hospitalization). Here, we report a detailed genomic characterization of this outbreak.

RESULTS

Data set characterization. During the first COVID-19 wave, an increase in incidence of *A. baumannii* strains was registered in the study hospital; the cases raised from a baseline of less than one isolate per 1,000 days of hospitalization in the 2018–2019 biennium to 2.8 isolates during the outbreak. We characterized 96 strains collected in this period (from January to July 2020) from 41 individuals hospitalized in the ICUs ($n = 37$), pneumology ($n = 2$), and otorhinolaryngology ($n = 1$) wards. Three samples were collected from one patient who was hospitalized in another care institute in Pavia (2 samples) and later admitted to the emergency department of the study hospital (1 sample). Patients had a mean age of 61 (standard deviation [SD], ± 10 years), ranging from 30 to 83 years old, and were predominantly male (87.8%; $n = 36$). The median length of stay was 47 days (interquartile range [IQR], 25 to 74 days), and 43.9% ($n = 18$) of patients died (median length of stay, 52 days; IQR, 37 to 85 days). Thirty patients tested positive and seven negative for SARS-CoV-2; the remaining four were

hospitalized before the pandemic period. Of the *A. baumannii* isolates, 33.3% ($n = 32$) were related to lower respiratory tract infections and 22.9% ($n = 22$) to bloodstream infections; 3.1% of strains were isolated from the urinary tract ($n = 3$) and the other 40.6% from rectal swabs ($n = 38$) and nasal swab ($n = 1$). Table S1 in the supplemental material summarizes isolate and patient information.

All 96 isolates were sequenced using both long- and short-read technology. The hybrid assemblies enabled us to obtain 8 complete and 87 high-quality genomes (mean length of the genomes, 4 Mbp; mean number of contigs, 11.3 (Table S2)). The remaining one was discarded (sample 4964_2020) and excluded from all downstream analyses. Genome analysis revealed that all 95 isolates belonged to sequence type 2 (ST2), which is part of the globally disseminated international clone II (IC2) (9).

Phylogenetic analysis. In order to further characterize the outbreak, we performed a phylogenetic analysis using the 95 *A. baumannii* genomes from the outbreak, 23 from the hospital surveillance program, and 367 from the PATRIC database as background. The inferred phylogeny (Fig. 1) depicts a situation in which the *A. baumannii* outbreak in the hospital was caused by multiple strains. The majority of the outbreak isolates ($n = 93$) are divided into two monophyletic clades, one larger (cluster 1; 71 outbreak strains in a clade of 80 total genomes; single nucleotide polymorphism (SNP) distance among cluster 1 genomes, 0 to 100) and one smaller (cluster 2; 23 outbreak strains; SNP distance among cluster 2 genomes, 0 to 43). Cluster 1 also includes nine isolates from the hospital surveillance program (one from 2019, four from 2020, and four from 2021) and one from the PATRIC DB. Cluster 2 is exclusively composed of 2020 isolates; nonetheless, isolate 4200_2019 from 2019 is basal to this cluster. A background isolate from Belgium (470.13595 of PATRIC DB) interposes between the 2019 surveillance isolate and cluster 2; however, the common branch to these genomes has very limited support (29/100 bootstraps). We measured the SNP distance between all genomes of cluster 1 and each one of cluster 2, which ranged between 274 and 356.

Interestingly, the genome of one of the two isolates from January 2020 not included in the main clusters (4636_2020) formed a monophyletic group with four 2019 surveillance genomes, while the second one (4614_2020) clustered with one surveillance genome from late 2020.

Antibiotic resistance and virulence. All 95 outbreak isolates were resistant to carbapenems (100% to imipenem and meropenem). Almost all isolates that presented resistance to aminoglycosides: 97.9% ($n = 93$) were found to be resistant to gentamicin and 98.9% ($n = 94$) to amikacin. Moreover, only 8.9% ($n = 7$) of isolates tested were resistant to tigecycline, and eight isolates were susceptible with increased exposure to this antibiotic. Additionally, the totality of isolates tested for ciprofloxacin ($n = 90$) were resistant. None of the isolates was found resistant to colistin. The antibiotic resistance factors predicted in the genomes were concordant with the phenotypes. Resistance to carbapenems was confirmed by the presence of *bla*_{OXA-23}. The intrinsic *bla*_{OXA-51}-variant, *bla*_{OXA-66}, was also detected, but no ISAb1 sequence insertion was found upstream. All strains carried a gene of the *bla*_{ADC-25} family: the majority ($n = 89$) presented *bla*_{ADC-73}, another five presented *bla*_{ADC-56}, and the remaining one had *bla*_{ADC-30} (Table S3).

Virulence determinants were also found in outbreak isolates, particularly those involved in biofilm formation. In detail, all isolates presented the *ompA* gene, which is important for the development of robust biofilms on abiotic surfaces (10), and the *bap* gene, which ensures a strong biofilm formation (11). Ninety-four out of 95 isolates had *csuA/B*, *csuA*, *csuB*, *csuC*, *csuD*, and *csuE* that encode the Chaperone-Usher secretion (CUS) system, fundamental for the first bacterial attachment on abiotic surfaces (12). The sole strain not carrying the CUS system was isolated in January 2020 (4614_2020).

Strains also had genes for BfmS/BfmR, a two-component system that plays a key role in CUS system regulation and *ompA* (13). Finally, 23.3% ($n = 25$) of the isolates presented the entire cluster of four genes (*pgaA*, *pgaB*, *pgaC*, and *pgaD*) responsible for the production of poly- β -(1,6)-*N*-acetylglucosamine (PNAG), a component of biofilm (12). Interestingly, these isolates included two from January 2020 (4636_2020, 4614_2020)

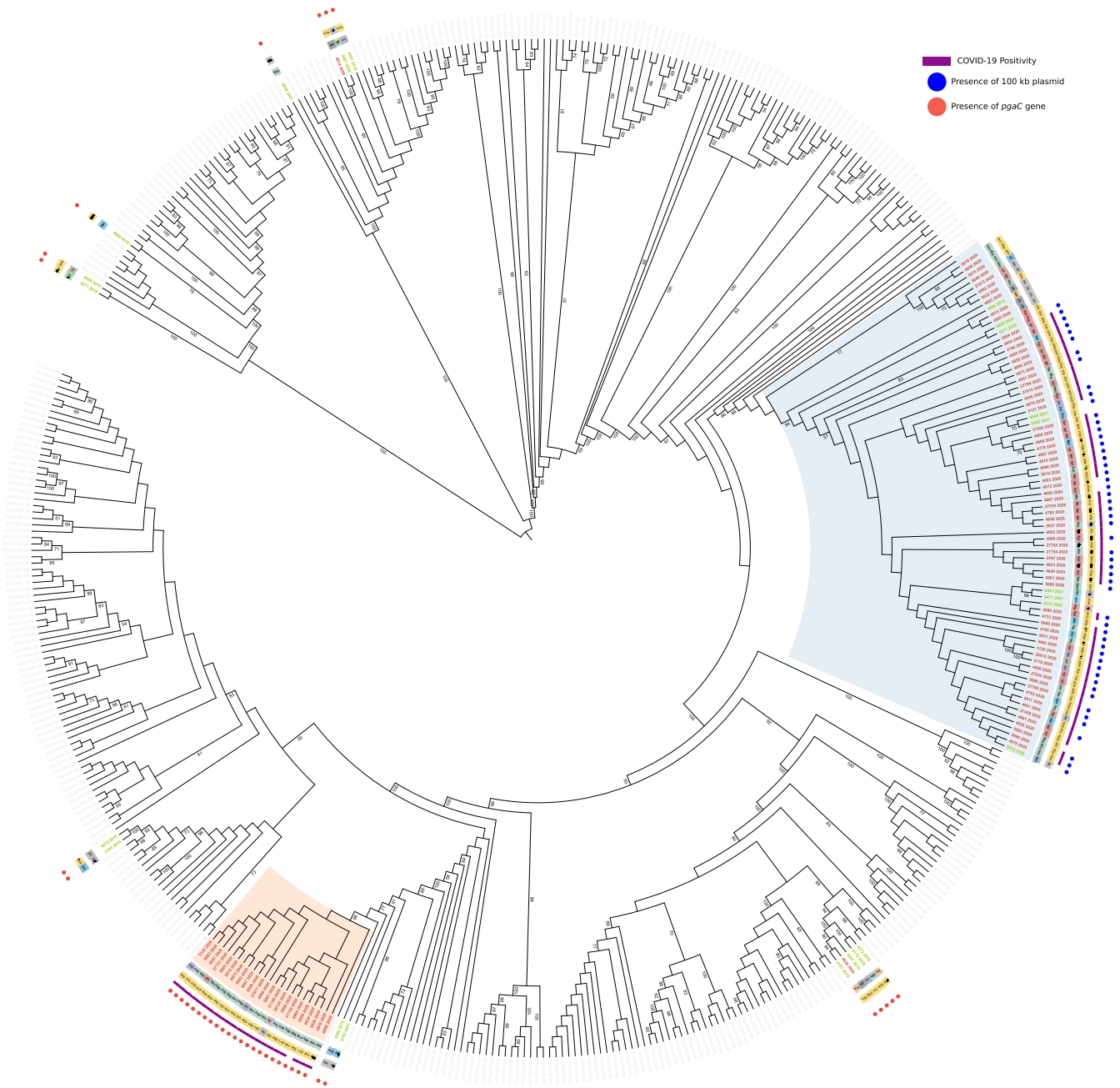


FIG 1 Maximum-likelihood phylogeny of 485 *A. baumannii* strains, including 95 outbreak genomes (red labels), 23 surveillance genomes (green labels), and 367 PATRIC genomes (gray labels) inferred on coreSNPs with RAxML. Date of isolation (innermost crown), ward (second crown), and SARS-CoV-2 positivity (third crown) were retrieved from the hospital and microbiological database. The presence of 100-kbp plasmid (blue dots) and *pgaC* gene (red dots) were determined by genomic analyses. The two main outbreak clusters are highlighted in blue (cluster 1) and red (cluster 2). Bootstrap values above 50/100 are indicated on tree branches. This figure was obtained using iTol (<https://itol.embl.de/>).

and those in cluster 2. In cluster 1 genomes ($n = 70$), the *pgaC* gene was instead interrupted by the ISAbA1 insertion sequence (Table S4).

Outbreak strains and those from the genomic surveillance program were tested for biofilm formation capability. The majority ($n = 64$) were found to be weak biofilm producers, while 40 were moderate producers, 13 strong producers, and only 1 was not a biofilm producer (Fig. S1). Interestingly, the isolates in the two large phylogenetic clusters tended to produce a weaker biofilm than the other isolates described in this work: in cluster 1, 67.50% are classified as weak, 28.75% are moderate, and 3.75% are strong producers; in cluster 2, 43.48% are weak producers, 47.82% are moderate, and 8.70%

are strong; and the remaining isolates are 6.66% nonproducers, 6.66% weak, 33.33% moderate, and 53.33% strong producers.

Plasmids. We investigated the presence of plasmids in the outbreak genomes and found that all the samples shared a plasmid of 8,731 bp, which perfectly matches GenBank accession no. [NZ_CP008708](#) containing 12 coding sequences, 10 being hypothetical proteins. Most of the genomes of cluster 1 (51/71) presented also a second, 106,175-bp-long, plasmid (highly similar to GenBank accession no. [CP081146](#)). Neither of the two plasmids encoded known virulence or resistance genes. We analyzed the ~100-kbp plasmid in depth; 83 out of its 131 coding sequences were annotated as hypothetical, 20 of which were reported to be phage associated. Indeed, the majority of the plasmid sequence consisted of a prophagic region of ~85 kbp (9261 to 95595). The phylogeny in Fig. 1 indicates that this plasmid is present only in cluster 1. Genomes in the basal position of the cluster do not carry the plasmid, suggesting that it was acquired with a single transfer event at the beginning of the outbreak. Also, the pattern of plasmid presence within the cluster indicates multiple losses. Lastly, we investigated the presence of the ~8-kbp and the ~100-kbp plasmids among the overall *A. baumannii* population ($n = 8,969$ genomes) and found them to be differentially distributed (Fig. S2). The first one was present in 32.1% ($n = 2,882$), and the second one was in 7% ($n = 636$) of the population.

DISCUSSION

In this work, we present the data from a hospital-wide outbreak of MDR *A. baumannii* that occurred during the first wave of the COVID-19 pandemic. A rise in the incidence of HAIs during COVID-19 pandemic waves was observed in the study hospital and also in other hospitals and countries worldwide (14–16). This is particularly true for *A. baumannii*, which was the most frequently reported cause of hospital outbreaks, together with methicillin-resistant *Staphylococcus aureus* and fungal infections (17–19). For example, during the first wave, Perez et al. reported a hospital-acquired carbapenem-resistant *A. baumannii* (CRAB) outbreak of 34 isolates harboring *bla*_{OXA-23r}, which involved 34 COVID-19 patients admitted to ICUs in New Jersey hospital (7). Also, Gottesman and colleagues (8) reported an outbreak in Israel of five CRAB carrying *bla*_{OXA-24} and belonging to IC2 in ICUs patients.

In our study, we were able to identify two large phylogenetic clusters (Fig. 1), which included most of the outbreak strains. The inclusion of genomes sequenced before and after the outbreak by the hospital surveillance program revealed that multiple strains were circulating in the hospital before the start of the pandemic, including the two (3996_2019 and 4200_2019) that caused the outbreak.

We detected two plasmids within our genomes, one of ~8 kbp and another of ~100 kbp. The second one is specific to a subclade of cluster 1 and contains a large prophage sequence carrying mostly uncharacterized genes. Four strains (4682_2020, 3996_2019, 4615_2020, and 4669_2020), which are basal to the subclade, were isolated in 2019 and early 2020, and their genomes did not contain the ~100-kbp plasmid. This suggests that the plasmid was acquired later during the outbreak, possibly within the hospital. The hypothesis is reinforced by the presence of another subclade of this cluster (n genomes = 8) in which the plasmid is absent. Moreover, this phage-encoding plasmid is supposedly specific to *A. baumannii*, as it is not present in other species (BLASTN on the nucleotide [nt] database performed on 4 October 2022). This observation suggests that the source of acquisition could have been another strain of *A. baumannii*, not detected by our surveillance program. Despite its fitness advantage not being clear, we can observe a tendency to preserve the plasmid in the genomes analyzed. This trend can be observed both in the local phylogeny (Fig. 1) and in the global one (see Fig. S2 in the supplemental material).

Mapping patient information on the tree revealed that SARS-CoV-2 coinfection was approximately equally distributed between the two phylogenetic clusters. Thus, no association between *A. baumannii* clusters and viral infection can be hypothesized. The

possibility of transmission of *A. baumannii* between COVID-19-positive and -negative patients in the absence of viral cotransmission is interesting and can be explained by the high capability of *A. baumannii* to survive on abiotic surfaces due to biofilm formation (20). In turn, this could also explain why this bacterial species thrived during the emergency period, both in the study hospital and in other institutions worldwide. Moreover, no association was found between clusters and wards, outcome, or age of patients.

The phylogeny we inferred allowed us to identify eight separate clusters of study genomes (including the two large ones), four of which contained strains isolated months before and after the epidemic event. This observation unveils the presence of at least four endemic clones in the study hospital, two of which gave origin to the large outbreak described in this work. Interestingly, no genomic factor that is known to enhance bacterial spread was found in the study genomes. Moreover, the biofilm formation capability of the isolates in the two large clusters was generally weaker than that of the other isolate described in this work (Fig. S1). This further suggests that the strains responsible for the outbreak did not have peculiar characteristics which could have favored their proliferation. In the genomes of cluster 1, we observed the interruption of the *pgaC* gene by the mobile element *ISAbal1*. This gene contributes to the formation of PNAG (21), and it was observed that the inactivation of this gene leads to a weaker adhesion capability in *Klebsiella pneumoniae* (22). In our work, we observed that the isolates in cluster 1 tend to be weaker biofilm producers than all others (including those in cluster 2), which have a functional *pgaC* gene. Cluster 1 is the largest, and it possibly includes the most diffusive clone in this study. Yet this cannot be attributed to a peculiar biofilm production capability. All in all, these results indicate that the spread of the bacterial pathogen was enhanced solely by the extreme emergency situation caused by the first wave of the COVID-19 pandemic. Personnel and bed shortages, and the prioritization of self-preservation from the viral infection of health care workers, led to unavoidable diminished attention toward the standard patient-handling measures (e.g., changing gloves between patients). In accordance with this hypothesis, the incidence of *A. baumannii* decreased to lower than 1 isolate per 1,000 days of hospitalizations after the first pandemic wave and remained under control during the following waves, thanks to better management of COVID-19 patients and a better knowledge of the viral disease.

MATERIALS AND METHODS

Data collection. This retrospective study was conducted at IRCCS Fondazione Policlinico San Matteo in Pavia (Italy), where 151 isolates of *A. baumannii* were collected from 6 January 2020 to 30 July 2020. Ninety-six isolates were chosen for use in this study; the choice was made favoring the inclusion of both samples from colonization and infection materials for each patient (where available) and of multiple samples in case of long hospitalizations (1 sample/7 days/material). The isolates selected were identified with matrix-assisted laser desorption ionization–time of flight mass spectrometry (MALDI-TOF MS; Bruker Daltonik, Bremen, Germany) equipped with Bruker Biotyper 3.1 software. Antibiotic susceptibility was tested with both the Sensititre Gram-negative EUMDROXF plate (Thermo Fisher Scientific, Rodano, Italy) and Phoenix NMIC-402 panel loaded on a BD Phoenix M50 instrument. Values were interpreted according to the European Committee on Antimicrobial Susceptibility Testing (EUCAST) clinical breakpoints (23). Tigecycline was interpreted following Clinical and Laboratory Standards Institute (CLSI) breakpoints (24).

Patient information was retrieved from the hospital database. COVID-19 positivity was defined at the time of admission, consulting the results of real-time reverse transcriptase PCR tests for the presence of SARS-CoV-2.

DNA extraction and genome characterization. The genomic DNA of the 96 strains was extracted with DNeasy blood and tissue kit (Qiagen) for short-read sequencing using an Illumina platform and with MagAttract high-molecular-weight (HMW) DNA kit (Qiagen) for long-read sequencing using Nanopore technology. Short and long reads were combined with the Unicycler software (25) to perform hybrid assemblies. The genomes obtained were then *in silico* sequence typed (ST) using the Pasteur multilocus sequence typing (MLST) scheme (26) with an in-house script. The presence of virulence and resistance genes was assessed using ABRicate (<https://github.com/tseemann/abricate>) with the NCBI AMRFinderPlus (27), CARD (28), Resfinder (29), and VirulenceFinder (30) databases. Results were manually curated and double-checked using BLAST and long reads. The presence of insertion sequences was determined with MobileElementFinder (31).

The presence of plasmids was evaluated with PlasmidFinder (32), and a more in-depth plasmid search was performed by visualizing the assembly graph in Bandage (33) for the least fragmented isolates, checking for circularity and higher depth coverage. The presence of the plasmids identified was

assessed in all the remaining assemblies using BLASTN. Plasmids were annotated combining Prokka (34), NCBI Conserved Domain Database (35), and possibly blastp on the nonredundant (nr) database. PHASTER (36) was then used to identify and annotate prophage sequences. In order to understand the prevalence of the plasmids found with our approach in the *A. baumannii* overall population, we created a collection of *A. baumannii* genomes, joining those from this study and all high-quality genomes from the PATRIC DB (sequences were retrieved in July 2022, using the makepordb.py script of the P-DOR pipeline [<https://github.com/SteMIDfactory/P-DOR>]). All assemblies were then scanned for the presence of all plasmid genes; genomes were considered to carry a plasmid when they encoded the vast majority of its genes (≥ 11 genes for the ~ 8 kbp; ≥ 120 genes for the ~ 100 kbp). Finally, FastTree (37) was used to infer the global phylogeny of the species, thus allowing us to study the distribution of the plasmids among the population.

Surveillance program genomes. Strains selected by the genomic surveillance program of the hospital are routinely processed for short-read sequencing as follows: DNA is extracted using DNeasy blood and tissue kit (Qiagen), sequenced with an Illumina platform, and assembled using Unicycler (25) with default parameters. We retrieved all the ST2 genomes obtained by the surveillance program ($n = 23$) in the months before and after the outbreak period (12 from 2019, 5 from 2020, and 6 from 2021), and we added them to our data set.

Biofilm formation assay. All *A. baumannii* isolates ($n = 119$) were tested for the ability to produce biofilm following the protocol described by Kumari and colleagues (38). *Pseudomonas aeruginosa* ATCC 27853 and *Staphylococcus epidermidis* 30678 from the internal laboratory collection (characterized to be a strong biofilm producer) were used as positive controls. Sterile medium was used as a negative control. Interpretation of optical density (OD) measurements was performed as previously described in reference 39. In detail, the cutoff value (c) was calculated as three standard deviations (SDs) above the average optical density (OD) of the negative control. Strains were classified into the following four categories based upon mean OD values: “no producer” when mean OD is $\leq c$, “weak producer” when c is less than the mean OD, which is $\leq 2c$, “moderate producer” when $2c$ is less than the mean OD, which is $\leq 4c$, and “strong producer” when mean OD is $> 4c$.

Phylogenetic analyses. In order to characterize the outbreak of *A. baumannii*, a genomic background was constructed. In detail, the 20 high-quality genomes most similar to those in our set according to k-mer content similarity (MASH [40]) were retrieved from the PATRIC DB (<https://www.patricbrc.org>). Then, the P-DOR pipeline (<https://github.com/SteMIDfactory/P-DOR>; version beta1.5) was used to align all genomes in our data set to an internal reference (the complete genome of strain 4946) and to extract core SNPs. Maximum-likelihood phylogeny was inferred with RAxML (41) (using 100 bootstraps resamples) on the resulting core SNP alignment using the general time reversible model, as suggested by ModelTest-NG (42), with ascertainment bias correction (43).

Ethical statement. The study was designed and conducted in accordance with the Helsinki Declaration and approved by the Ethics Committee of Fondazione IRCCS Policlinico San Matteo in Pavia, Italy (internal project code, 08022298/13; project number 733-rcr2013-34). The work described herein is a retrospective study performed on bacterial isolates from human samples that were obtained as part of routine hospital care.

Data availability. Assembled genomes of outbreak and surveillance *A. baumannii* isolates are deposited in the National Center for Biotechnology Information (NCBI) under the BioProject accession no. PRJNA844013.

SUPPLEMENTAL MATERIAL

Supplemental material is available online only.

SUPPLEMENTAL FILE 1, XLSX file, 0.1 MB.

SUPPLEMENTAL FILE 2, XLSX file, 0.05 MB.

SUPPLEMENTAL FILE 3, XLSX file, 0.1 MB.

SUPPLEMENTAL FILE 4, XLSX file, 0.1 MB.

SUPPLEMENTAL FILE 5, PDF file, 1 MB.

ACKNOWLEDGMENTS

We acknowledge Anna K. Pöntinen and Francois Cleon for experimental assistance and the Genomics Support Centre Tromsø, UiT The Arctic University of Norway, for the short- and long-read sequencing.

J.C. was supported by ERC grant 742158. S.G. was supported by Ricerca Corrente grant 924-rcr2018i-34 (Italian Ministry of Health).

REFERENCES

1. Lob SH, Hoban DJ, Sahm DF, Badal RE. 2016. Regional differences and trends in antimicrobial susceptibility of *Acinetobacter baumannii*. *Int J Antimicrob Agents* 47:317–323. <https://doi.org/10.1016/j.ijantimicag.2016.01.015>.
2. Yang C-H. 2022. WHO regional office for Europe/European centre for disease prevention and control. antimicrobial resistance surveillance in Europe 2022 to 2020 data. WHO Regional Office for Europe, Copenhagen, Denmark.
3. Yang C-H, Su P-W, Moi S-H, Chuang L-Y. 2019. Biofilm formation in *Acinetobacter baumannii*: genotype-phenotype correlation. *Molecules* 24:1849. <https://doi.org/10.3390/molecules24101849>.

4. Antunes LCS, Visca P, Towner KJ. 2014. *Acinetobacter baumannii*: evolution of a global pathogen. *Pathog Dis* 71:292–301. <https://doi.org/10.1111/2049-632X.12125>.
5. Wong D, Nielsen TB, Bonomo RA, Pantapalangkoor P, Luna B, Spellberg B. 2017. Clinical and pathophysiological overview of *Acinetobacter* infections: a century of challenges. *Clin Microbiol Rev* 30:409–447. <https://doi.org/10.1128/CMR.00058-16>.
6. Tacconelli E, Carrara E, Savoldi A, Harbarth S, Mendelson M, Monnet DL, Pulcini C, Kahlmeter G, Kluytmans J, Carmeli Y, Ouellette M, Outterson K, Patel J, Cavalieri M, Cox EM, Houchens CR, Grayson ML, Hansen P, Singh N, Theuretzbacher U, Magrini N, WHO Pathogens Priority List Working Group. 2018. Discovery, research, and development of new antibiotics: the WHO priority list of antibiotic-resistant bacteria and tuberculosis. *Lancet Infect Dis* 18:318–327. [https://doi.org/10.1016/S1473-3099\(17\)30753-3](https://doi.org/10.1016/S1473-3099(17)30753-3).
7. Perez S, Innes GK, Walters MS, Mehr J, Arias J, Greeley R, Chew D. 2020. Increase in hospital-acquired carbapenem-resistant *Acinetobacter baumannii* infection and colonization in an acute care hospital during a surge in COVID-19 admissions—New Jersey, February–July 2020. *MMWR Morb Mortal Wkly Rep* 69:1827–1831. <https://doi.org/10.15585/mmwr.mm6948e1>.
8. Gottesman T, Fedorowsky R, Yerushalmi R, Lellouche J, Nutman A. 2021. An outbreak of carbapenem-resistant *Acinetobacter baumannii* in a COVID-19 dedicated hospital. *Infect Prev Pract* 3:100113. <https://doi.org/10.1016/j.infpip.2021.100113>.
9. Dijkshoorn L, Aucken H, Gerner-Smidt P, Janssen P, Kaufmann ME, Garaizar J, Ursing J, Pitt TL. 1996. Comparison of outbreak and nonoutbreak *Acinetobacter baumannii* strains by genotypic and phenotypic methods. *J Clin Microbiol* 34:1519–1525. <https://doi.org/10.1128/jcm.34.6.1519-1525.1996>.
10. Gaddy JA, Tomaras AP, Actis LA. 2009. The *Acinetobacter baumannii* 19606 *OmpA* protein plays a role in biofilm formation on abiotic surfaces and in the interaction of this pathogen with eukaryotic cells. *Infect Immun* 77:3150–3160. <https://doi.org/10.1128/IAI.00096-09>.
11. Azizi O, Shahcheraghi F, Salimzand H, Modarresi F, Shakibaie MR, Mansouri S, Ramazanzadeh R, Badmasti F, Nikbin V. 2016. Molecular analysis and expression of *bap* gene in biofilm-forming multi-drug-resistant *Acinetobacter baumannii*. *Rep Biochem Mol Biol* 5:62–72.
12. Tomaras AP, Dorsey CW, Edelmann RE, Actis LA. 2003. Attachment to and biofilm formation on abiotic surfaces by *Acinetobacter baumannii*: involvement of a novel chaperone-usher pili assembly system. *Microbiology (Reading)* 149:3473–3484. <https://doi.org/10.1099/mic.0.26541-0>.
13. Kishii K, Hamada M, Aoki K, Ito K, Onodera J, Ishii Y, Tateda K. 2020. Differences in biofilm formation and transcription of biofilm-associated genes among *Acinetobacter baumannii* clinical strains belonging to the international clone II lineage. *J Infect Chemother* 26:693–698. <https://doi.org/10.1016/j.jiac.2020.02.017>.
14. Garcia-Vidal C, Sanjuan G, Moreno-García E, Puerta-Alcalde P, Garcia-Pouton N, Chumbita M, Fernandez-Pittol M, Pitart C, Inciarte A, Bodro M, Morata L, Ambrosioni J, Grafía I, Meira F, Macaya I, Cardozo C, Casals C, Tellez A, Castro P, Marco F, García F, Mensa J, Martínez JA, Soriano A, COVID-19 Researchers Group. 2021. Incidence of co-infections and superinfections in hospitalized patients with COVID-19: a retrospective cohort study. *Clin Microbiol Infect* 27:83–88. <https://doi.org/10.1016/j.cmi.2020.07.041>.
15. Cusumano JA, Dupper AC, Malik Y, Gavioli EM, Banga J, Berbel Caban A, Nadkarni D, Obla A, Vasa CV, Mazo D, Altman DR. 2020. *Staphylococcus aureus* bacteremia in patients infected with COVID-19: a case series. *Open Forum Infect Dis* 7:ofaa518. <https://doi.org/10.1093/ofid/ofaa518>.
16. Contou D, Claudinon A, Pajot O, Micaëlo M, Longuet Flandre P, Dubert M, Cally R, Logre E, Fraissé M, Mentec H, Plantefève G. 2020. Bacterial and viral co-infections in patients with severe SARS-CoV-2 pneumonia admitted to a French ICU. *Ann Intensive Care* 10:119. <https://doi.org/10.1186/s13613-020-00736-x>.
17. Pascale R, Bussini L, Gaibani P, Bovo F, Fornaro G, Lombardo D, Ambretti S, Pensalfine G, Appolloni L, Bartoletti M, Tedeschi S, Tumietto F, Lewis R, Viale P, Giannella M. 2022. Carbapenem-resistant bacteria in an intensive care unit during the coronavirus disease 2019 (COVID-19) pandemic: a multicenter before-and-after cross-sectional study. *Infect Control Hosp Epidemiol* 43:461–466. <https://doi.org/10.1017/ice.2021.144>.
18. O'Toole RF. 2021. The interface between COVID-19 and bacterial health-care-associated infections. *Clin Microbiol Infect* 27:1772–1776. <https://doi.org/10.1016/j.cmi.2021.06.001>.
19. Kundu R, Singla N. 2022. COVID-19 and plethora of fungal infections. *Curr Fungal Infect Rep* 16:47–54. <https://doi.org/10.1007/s12281-022-00432-2>.
20. Eze EC, Chenia HY, El Zowalaty ME. 2018. *Acinetobacter baumannii* biofilms: effects of physicochemical factors, virulence, antibiotic resistance determinants, gene regulation, and future antimicrobial treatments. *Infect Drug Resist* 11:2277–2299. <https://doi.org/10.2147/IDR.S169894>.
21. Choi AHK, Slamti L, Avci FY, Pier GB, Maira-Litrán T. 2009. The *pgaABC*D locus of *Acinetobacter baumannii* encodes the production of poly-beta-1-6-N-acetylglucosamine, which is critical for biofilm formation. *J Bacteriol* 191:5953–5963. <https://doi.org/10.1128/JB.00647-09>.
22. Chen K-M, Chiang M-K, Wang M, Ho H-C, Lu M-C, Lai Y-C. 2014. The role of *pgaC* in *Klebsiella pneumoniae* virulence and biofilm formation. *Microb Pathog* 77:89–99. <https://doi.org/10.1016/j.micpath.2014.11.005>.
23. The European Committee on Antimicrobial Susceptibility Testing. 2020. Breakpoint tables for interpretation of MICs and zone diameters. version 10.0.
24. Clinical and Laboratory Standards Institute. 2020. Performance Standards for Antimicrobial Susceptibility Testing. CLSI, CLSI supplement M100, 30th ed, Wayne, PA.
25. Wick RR, Judd LM, Gorrie CL, Holt KE. 2017. Unicycler: resolving bacterial genome assemblies from short and long sequencing reads. *PLoS Comput Biol* 13:e1005595. <https://doi.org/10.1371/journal.pcbi.1005595>.
26. Diancourt L, Passet V, Nemeč A, Dijkshoorn L, Bricse S. 2010. The population structure of *Acinetobacter baumannii*: expanding multiresistant clones from an ancestral susceptible genetic pool. *PLoS One* 5:e10034. <https://doi.org/10.1371/journal.pone.0010034>.
27. Feldgarden M, Brover V, Haft DH, Prasad AB, Slotta DJ, Tolstoy I, Tyson GH, Zhao S, Hsu C-H, McDermott PF, Tadesse DA, Morales C, Simmons M, Tillman G, Wasilenko J, Folster JP, Klimke W. 2019. Validating the AMRFinder tool and resistance gene database by using antimicrobial resistance genotype-phenotype correlations in a collection of isolates. *Antimicrob Agents Chemother* 63:e00483-19. <https://doi.org/10.1128/AAC.00483-19>.
28. Jia B, Raphenya AR, Alcock B, Waglechner N, Guo P, Tsang KK, Lago BA, Dave BM, Pereira S, Sharma AN, Doshi S, Courtot M, Lo R, Williams LE, Frye JG, Elsayegh T, Sardar D, Westman EL, Pawlowski AC, Johnson TA, Brinkman FSL, Wright GD, McArthur AG. 2017. CARD 2017: expansion and model-centric curation of the comprehensive antibiotic resistance database. *Nucleic Acids Res* 45:D566–D573. <https://doi.org/10.1093/nar/gkw1004>.
29. Zankari E, Hasman H, Cosentino S, Vestergaard M, Rasmussen S, Lund O, Aarestrup FM, Larsen MV. 2012. Identification of acquired antimicrobial resistance genes. *J Antimicrob Chemother* 67:2640–2644. <https://doi.org/10.1093/jac/dks261>.
30. Joensen KG, Scheutz F, Lund O, Hasman H, Kaas RS, Nielsen EM, Aarestrup FM. 2014. Real-time whole-genome sequencing for routine typing, surveillance, and outbreak detection of verotoxigenic *Escherichia coli*. *J Clin Microbiol* 52:1501–1510. <https://doi.org/10.1128/JCM.03617-13>.
31. Johansson MHK, Bortolaia V, Tansirichaiya S, Aarestrup FM, Roberts AP, Petersen TN. 2021. Detection of mobile genetic elements associated with antibiotic resistance in *Salmonella enterica* using a newly developed web tool: MobileElementFinder. *J Antimicrob Chemother* 76:101–109. <https://doi.org/10.1093/jac/dkaa390>.
32. Carattoli A, Zankari E, García-Fernández A, Voldby Larsen M, Lund O, Villa L, Møller Aarestrup F, Hasman H. 2014. In silico detection and typing of plasmids using PlasmidFinder and plasmid multilocus sequence typing. *Antimicrob Agents Chemother* 58:3895–3903. <https://doi.org/10.1128/AAC.02412-14>.
33. Wick RR, Schultz MB, Zobel J, Holt KE. 2015. Bandage: interactive visualization of de novo genome assemblies. *Bioinformatics* 31:3350–3352. <https://doi.org/10.1093/bioinformatics/btv383>.
34. Seemann T. 2014. Prokka: rapid prokaryotic genome annotation. *Bioinformatics* 30:2068–2069. <https://doi.org/10.1093/bioinformatics/btu153>.
35. Marchler-Bauer A, Lu S, Anderson JB, Chitsaz F, Derbyshire MK, DeWeese-Scott C, Fong JH, Geer LY, Geer RC, Gonzales NR, Gwadz M, Hurwitz DI, Jackson JD, Ke Z, Lanczycki CJ, Lu F, Marchler GH, Mullokandov M, Omelchenko MV, Robertson CL, Song JS, Thanki N, Yamashita RA, Zhang D, Zhang N, Zheng C, Bryant SH. 2011. CDD: a Conserved Domain Database for the functional annotation of proteins. *Nucleic Acids Res* 39:D225–D229. <https://doi.org/10.1093/nar/gkq1189>.

36. Arndt D, Grant JR, Marcu A, Sajed T, Pon A, Liang Y, Wishart DS. 2016. PHASTER: a better, faster version of the PHAST phage search tool. *Nucleic Acids Res* 44:W16–21. <https://doi.org/10.1093/nar/gkw387>.
37. Price MN, Dehal PS, Arkin AP. 2009. FastTree: computing large minimum evolution trees with profiles instead of a distance matrix. *Mol Biol Evol* 26: 1641–1650. <https://doi.org/10.1093/molbev/msp077>.
38. Kumari M, Bhattarai NR, Rai K, Pandit TK, Khanal B. 2022. Multidrug-resistant *Acinetobacter*: detection of ESBL, MBL, blaNDM-1 genotype, and biofilm formation at a tertiary care hospital in eastern Nepal. *Int J Microbiol* 2022:8168000. <https://doi.org/10.1155/2022/8168000>.
39. Stepanović S, Vuković D, Hola V, Di Bonaventura G, Djukić S, Cirković I, Ruzicka F. 2007. Quantification of biofilm in microtiter plates: overview of testing conditions and practical recommendations for assessment of biofilm production by staphylococci. *APMIS* 115:891–899. https://doi.org/10.1111/j.1600-0463.2007.apm_630.x.
40. Ondov BD, Treangen TJ, Melsted P, Mallonee AB, Bergman NH, Koren S, Phillippy AM. 2016. Mash: fast genome and metagenome distance estimation using MinHash. *Genome Biol* 17:132. <https://doi.org/10.1186/s13059-016-0997-x>.
41. Stamatakis A. 2014. RAxML version 8: a tool for phylogenetic analysis and post-analysis of large phylogenies. *Bioinformatics* 30:1312–1313. <https://doi.org/10.1093/bioinformatics/btu033>.
42. Darriba D, Posada D, Kozlov AM, Stamatakis A, Morel B, Flouri T. 2020. ModelTest-NG: a new and scalable tool for the selection of DNA and protein evolutionary models. *Mol Biol Evol* 37:291–294. <https://doi.org/10.1093/molbev/msz189>.
43. Lewis PO. 2001. A likelihood approach to estimating phylogeny from discrete morphological character data. *Syst Biol* 50:913–925. <https://doi.org/10.1080/106351501753462876>.